AIAA JOURNAL
Vol. 45, No. 10, October 2007

# Technical Notes

*TECHNICAL NOTES are short manuscripts describing new developments or important results of a preliminary nature. These Notes should not exceed 2500 words (where a figure or table counts as 200 words). Following informal review by the Editors, they may be published within a few months of the date of receipt. Style requirements are the same as for regular contributions (see inside back cover).*

## Three-Dimensional Computational Simulation of Surface Corrosion Damage

Ramana M. Pidaparti*
*Virginia Commonwealth University, Richmond, Virginia 23284*
Anuj Puri† and Mathew J. Palakal‡
*Indiana University—Purdue University at Indianapolis, Indianapolis, Indiana 46202*
and
Ajay Kashyap§
*Indian Institute of Technology, Bombay 400 076, India*

DOI: 10.2514/1.18149

### Introduction

CORROSION is one of the degradation mechanisms in aerospace structures [1]. Among various types of corrosion, pitting corrosion associated with the dissolution of metal is caused by the breakdown of the passive film on the metal surface and is known to be one of the major damage mechanisms affecting the integrity of many aerospace structures. Pitting corrosion is a complex process, and a fundamental aspect of pitting corrosion failure mechanisms is that they tend to initiate at the micro/nanostructure level [2]. The details of the mechanisms vary with material composition, electrolyte, and other environmental conditions [3]. It is well known that pitting corrosion has a strong effect on the fatigue life of aluminum alloys used in aircraft structures [4–6]. Prediction of pitting corrosion damage is therefore very important for the structural integrity of aerospace materials and structures.

Although pitting corrosion has been studied extensively over the past two decades, computational modeling of pit initiation and growth is still open to investigation. Several pitting corrosion models exist in the literature [7–13] and are mostly empirical, mechanistic, deterministic, or phenomenological in nature. Pitting corrosion involves repassivation, mass transport, electrochemistry, and other mechanisms that operate at different length scales, thus making modeling a difficult problem. Recently, Burstein et al. [14] demonstrated that pit nucleation occurs at the microscopic level and is random in nature and that some metals show preferential sites of pit nucleation. Even though there are experimental studies aimed at understanding the basic mechanisms, the observed complexity is very difficult to interpret, with many controlled variables affecting the pitting process. In general, the corrosion damage modeling should involve not only physicochemical and environmental factors, but also various parameters, random in nature. Therefore, a more realistic computational corrosion damage model should integrate various parameters that are random in nature from electrochemistry, materials science, and probability and statistics. In contrast to mechanistic approaches, computational modeling of pitting corrosion based on local rules with evolving patterns may open up the possibility of getting insight into pitting corrosion from a different point of view. Recently, Pidaparti et al. [15] developed a two-dimensional model for studying pitting corrosion growth based on the cellular automata (CA) approach. However, they did not consider the initiation phase of pitting corrosion in their model.

The main objective of this work is to develop an approach to modeling three-dimensional surface-corrosion-damage initiation and growth using specific rules governing the electrochemical reactions in a cellular automata environment. The results of corrosion damage growth obtained from the three-dimensional model are compared with the experimental data obtained from the Center for Materials Diagnostics at the University of Dayton Research Institute.

### Corrosion-Pit Initiation-and-Growth Model

Pitting, in general, comprises three stages: pit initiation, metastable pit, and stable pit. Pit initiation is the first step of pitting, in which the passive film on the metal surface breaks down and the initiation of pitting takes place at random points on the metal surface. These initial pits require a suitable environment to grow into stable pits. The stage at which the pits may repassivate in case of an unsuitable environment is known as the metastable stage. If the proper conditions are satisfied, these initial pits grow into stable pits. These stable pits then grow and lead to the deterioration of the whole metal. Stable pit growth, in which the pit propagates effectively and indefinitely, is preceded by a metastable state. The metastable state of growth occurs when the pit is still very small, and its continued propagation to reach the stable state is not guaranteed. Many metastable pits die through repassivation while still in the metastable growth state. Metastable pits that do not achieve stability are not in themselves necessarily structurally damaging, although they affect surface finish on a microscopic scale. The proposed model takes into account both pit initiation and growth phases.

#### Governing Electrochemical Relations

It is important to consider the electrochemical reactions taking place during corrosion, along with the cellular automata rules described in the next section. This section describes the governing equations (1–5) used for the initiation and the growth of the corrosion model.

The first step in the pit initiation process is the formation of embryos. The nucleus of the pit is referred to as an embryo. Once the pit has nucleated, the embryo requires certain factors, both physical and environmental, to build up into a pit. The concept of embryos was introduced by Farmer et al. [16], among others, who used the term embryo to describe the first stage of pit initiation. Embryos denote the stage before the initiation step, in which they may survive or not, depending on several conditions. The birth of the embryos

Received 10 June 2005; revision received 1 June 2007; accepted for publication 1 June 2007. 

*Professor, Department of Mechanical Engineering, 601 West Main Street. Associate Fellow AIAA.
†Graduate Student, Department of Computer and Information Science, 723 West Michigan Street.
‡Professor, School of Informatics, Purdue School of Science, 723 West Michigan Street.
§Undergraduate Student, Department of Mechanical Engineering.

depends on $\lambda_1$, which is given by

$$\lambda_1 = \lambda_0[\mathrm{Cl}]\exp\left\langle\frac{\alpha_\lambda F}{RT}(E - E_{\mathrm{crit}})\right\rangle \tag{1}$$

where $\lambda_1$ is the birth probability, $\lambda_0$ is the intrinsic rate constant for birth of embryos, Cl is the chloride concentration of solution, $\alpha_\lambda$ is constant, $F$ is Faraday's constant, $R$ is the universal gas constant, $T$ is the absolute temperature, $E$ is the electrochemical potential applied to the surface, and $E_{\mathrm{crit}}$ is the critical potential over which pitting takes place.

Because the embryos have a tendency to repassivate if they are not provided with the right environmental conditions, a death probability occurs. In case the embryo satisfies the death probability, it repassivates. The death probability is given by

$$\mu_1 = \mu_0[\mathrm{OH}-]\exp\left\langle-\frac{\alpha_\mu F}{RT}(E - E_{\mathrm{pass}})\right\rangle \tag{2}$$

where $\mu_1$ is the death probability of the embryo, $\mu_0$ is the intrinsic constant for the death of the embryo, $OH^-$ is the concentration of hydroxyl anion, $\alpha_\mu$ is constant, and $E_{\mathrm{pass}}$ is the potential over/under which the embryo repassivates.

An assumption is made that if the probability exceeds one, depending on the environmental and chemical parameters, it is adjusted to one, which means that in the case of birth probability, each cell will corrode, whereas in the case of death probability, each cell will repassivate. Once the embryo is formed, the next stage is the transition from embryo to pit. This transition rate $\lambda_1$ is given by

$$\gamma_1 = \gamma_0\exp\left(-\frac{A_\gamma}{RT}\right) \tag{3}$$

where $\gamma_1$ is the transition rate from embryo to stable pit, $\gamma_o$ is the intrinsic rate constant, and $A_\gamma$ is the apparent activation energy.

The transition stage is actually the metastable stage, in which the pits are still in the initiation stage. They are still susceptible to repassivity and have not entered the growth stage. In a review of the temperature dependence of pit initiation, Szklarska-Smialowska [17] found considerable variability. Arrhenius behavior was not always observed, and the tendency for pitting was found both to increase and decrease with increasing temperature. Another variable that was considered in the present model is the induction time $\tau_1$, which is the age that an embryo must reach before it becomes a stable pit:

$$\tau_1 = \tau_0\exp\left(-\frac{A_\tau}{RT}\right) \tag{4}$$

where $\tau_1$ is the induction time, $\tau_0$ is the intrinsic induction time, $A_\tau$ is the apparent activation energy, and $T$ is the absolute temperature.

In the present model, the transition stage continues from 1 till 32. This pixel range of 1–32 is based on the fact that pit initiation life is about 10–25% of the pit growth life [1,2,6,12]. So in the simulation, we have taken 32 out of 255 pixels as the values for pit initiation, giving approximately 12.5% life. After the pit reaches a pixel value of 32, the pit enters the growth stage. At this stage, the pit cannot repassivate. The pit will continue to grow until the whole area of the metal gets completely corroded. The rate at which the growth will take place depends upon the local rules of the cellular automata, as described in the next section, along with the growth rate formula, given by

$$\ell_n\left(\frac{\Delta r}{\Delta t}\right) = 13.409 - \left(\frac{5558.7}{T + 273}\right) - 0.087(\mathrm{pH}) + 0.56965(\mathrm{conc}) \tag{5}$$

where $\Delta r/\Delta t$ is the growth rate of the pit, $T$ is the absolute temperature, pH is the pH of the solution, and conc is the concentration of the solution.

The electrochemical parameters such as potential, concentration, temperature, and pH differ for every cell in the cellular automata environment, which in turn changes the rates of transition and growth for each cell individually.

## Cellular Automata Rules and Simulation Algorithm

The corrosion pit initiation and growth behaviors were modeled as a discrete dynamic system using the cellular automata rules and the governing electrochemical equations. CA-based modeling techniques are powerful methods to describe, simulate, and understand the behavior of complex physical systems [18]. The original CA model [18] is a two-dimensional square lattice in which each square is called a *cell*. Each of these cells can be in a different state at any given time. The evolution of each cell and the updating of the internal states of each cell occur synchronously and are governed by a set of *rules*. The cellular space thus created is a complete discrete dynamic system. Earlier work by Wolfram [19,20] showed that the CA as a discrete dynamic system exhibits many of the properties of a continuous dynamic system, yet CA provide a simpler framework. The approach taken in this study is to slice the metal into layers at various depths, starting from the top surface of the metal, as shown in Fig. 1. The depth of the layers is chosen by the user through the simulation interface. The corrosion starts at the top surface and, with time, it spreads down into the metal. In the present simulation, a Moore neighborhood is considered for each surface layer in the metal. The

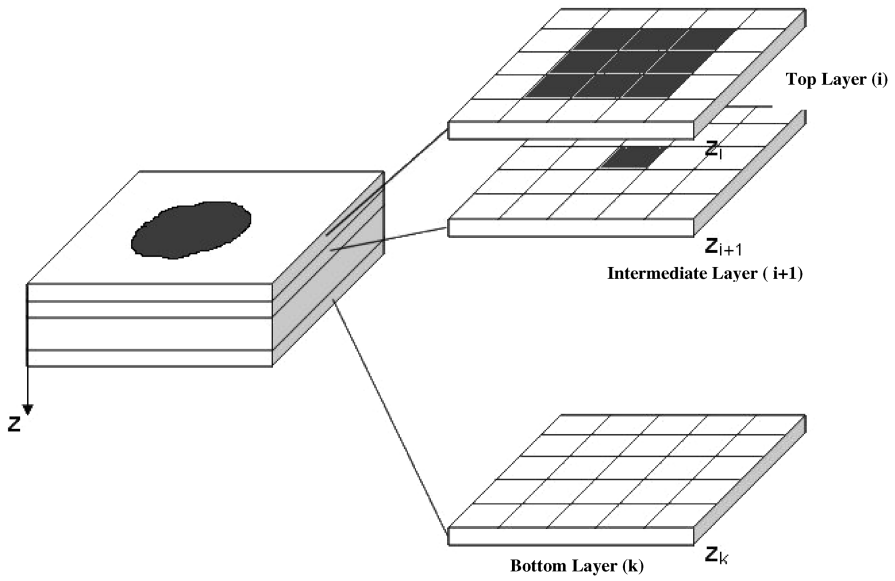


**Fig. 1 Computational approach to model three-dimensional surface corrosion in metals.**

Moore neighborhood is a square-shaped neighborhood that limits interactions of an individual to its eight neighbors that share a vertex or edge with the center cell. Figure 2 shows the flowchart of the corrosion damage algorithm and its implementation using the CA environment. The governing CA rules for pit initiation and growth are briefly described next.

### CA Rules for Pit Initiation

The cellular automata rules governing pit initiation are as follows:

1) The corrosion damage growth starts from the top surface of the material. The material is represented as layers of 2-D surfaces (a 2-D surface being a grid of rectangular cells). In general, each cell is affected by its adjoining 26 neighboring cells in three dimensions.

2) $S(u, t)$ and $E(u, t)$ are the initial states of an uncorroded and corroded cell $u$ at time $t$, respectively. The corroded cell $S(u, t)$ takes values between 1 and 32 based on the pixel values in the simulation. The state of $S(u, t) = 1$ means that the pit started to initiate, will continue until it reaches 32, and after that, the pit will follow the growth rules.

3) The birth-probability and death-probability rates [see Eqs. (1) and (2)] are set or varied according to the simulation.

4) For each simulated cycle, each uncorroded cell gets corroded according to the birth probability. In case the cells do not satisfy the birth-probability condition, for each uncorroded cell $S(u, t)$, the Moore neighborhood is considered. If more than four neighbors are embryos [$E(u, t)$ state], a corrosion pit is initiated at cell $u$ and its corrosion state $S(u, t)$ is set to one, which corresponds to the pit initiation stage.

5) For each corroded cell $E(u, t)$, the death probability is checked to see if a cell satisfies the death-probability condition. If yes, then the cell repassivates. A corroded cell needs at least one of its neighbors to be in the corroded state $E(u, t)$. If none of the neighbors is corroded, the cell repassivates and its state is set to $S(u, t)$.

6) For each corroded cell $E(u, t)$, if there is more than one neighbor with a corroded state, the transition rate is applied: $E(u, t + 1) = E(u, t) + r$, where $r$ is the transition rate according to the transition rate formula, as shown in Fig. 2. The transition rate takes place on cells with states between 4 and 32 for pit initiation. This threshold is based on the pixel values (1–255) and the time for pit initiation and growth processes [1–3].

7) For the next step, repeat step 2 on the uncorroded cells and repeat steps 3 and 4 on the corroded cells. According to the simulation, the pits may continue to die until they reach state 4. After $E(u, t)$ becomes more than four, the pits cannot die, but they enter the metastable state. If the pits reach state 32, they finally initiate. At this stage, the pit growth algorithm of Fig. 2 and Eq. (5) is applied on the corresponding cells.

In the initiation stage, the pits are in a metastable state; that is, in cases in which they are not provided with the ideal conditions necessary for corrosion, they may die or repassivate. The metastable pits do not grow according to the formulas governing the growth rate, but are dependent on the transition rate. Once a pit reaches $E(u, t)$ of 32, it reaches the stable pit criterion and is then governed by the growth model equations. In general, the propagation stage of pitting is characterized by several important aspects: current distribution in and around pits, potential distribution in and around pits, electrolyte composition within pits, the morphology of pitting (size, shape, and distribution of pits), and the kinetics of pit propagation. In this study, the growth rate formula, which relates the pit growth to pH, electrolyte concentration, and the absolute temperature, along with the following rules, are implemented in the simulation.

### CA Rules for Pit Growth

1) The cell in which a pit has initiated acquires state $C(u, t)$, which extends from 32 to 255. At the stage when $C(u, t)$ reaches 255, then the cell corrodes completely.

2) At each time step, a partial corroded cell becomes further corroded to a degree given by the pitting effects of the corroded cell on itself and of the corroded neighbors in the Moore neighborhood.

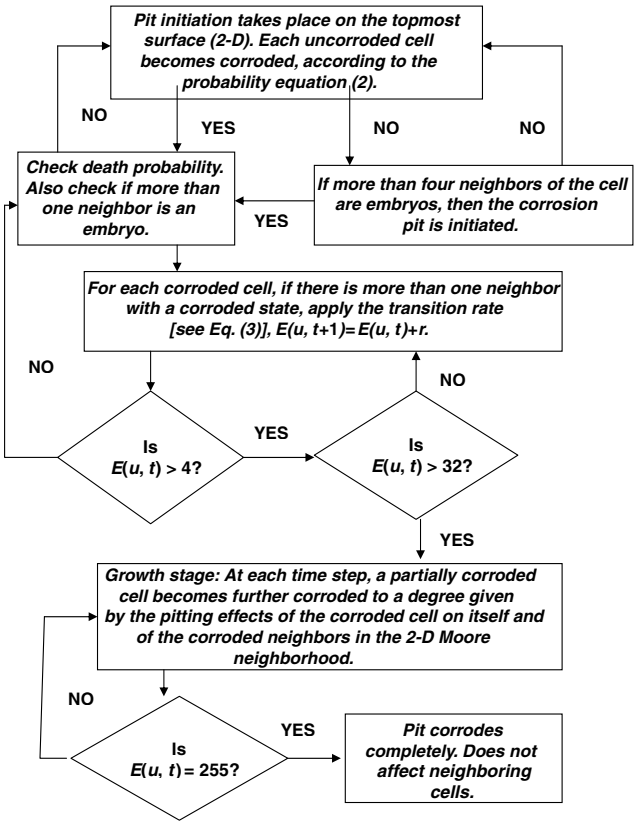


**Fig. 2 Flowchart of the CA implementation of the corrosion initiation and growth model.**

3) During the corrosion growth process, a fully corroded cell becomes an empty cell; that is, all the material is gone and it has a minimum effect on the corrosion of the neighboring cell.

## Results and Discussion

The cellular automata rules and electrochemical governing equations described in the previous sections were implemented by developing a computer program in an object-oriented programming with a JAVA environment. The developed computer program asks the user to enter the number of layers and the layer numbers through a user interface. The user can input the layer numbers they want to view, to check the extent of penetration of corrosion inside the metal. At present, the program is capable of displaying the four layers simultaneously, along with producing the numbers of births, deaths, and growths taking place in every single simulation cycle, as well as cumulatively. The variation in the sensitive parameters is also recorded, but the values at only the center of the pit are displayed.

To illustrate the corrosion pit initiation and growth processes, a simulation was run for 150 cycles with initial environmental parameters (pH $= 3.5$, $E = 0.6$ V, conc $= 290$ mol/dm$^{-3}$, and $T = 290$°F). A cross-boxed approach for displaying images was chosen to give a more realistic representation. Figure 3 shows the results of simulation at four intervals (cycles, $n = 70$, 85, 100, and 115). It can be seen from Fig. 3 that at the simulation cycle of 70, the pits are initiated and there are three and two distinct areas in which pits are initiated on the top two layers, respectively. With increasing time (cycles), the initiated pits are growing in size and new pits are also being initiated. As the cycles are increased, more pits initiate and grow, and finally at cycle 115, about 60–75% of the area is corroded. If we let the simulation continue for more cycles, the whole area will be corroded. It was observed that the distribution of potential over the surface is not uniform and nonhomogeneous. It is useful to know that corrosion initiation and growth is different over the surface and that many parameters affect corrosion differently. Usually, corrosion experiments are done in a cell, and not all the electrochemical

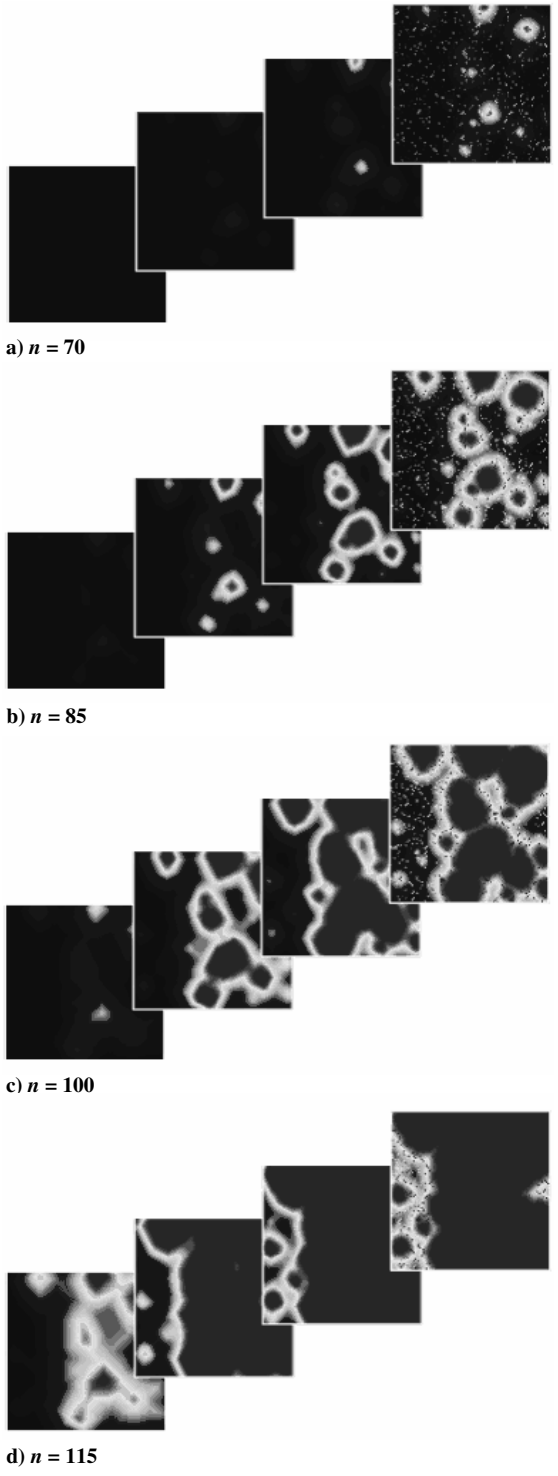


**Fig. 3 Computational simulation of the corrosion process at different cycles.**

parameters are monitored during the experiments. In such experimental cases, our simulation results should be helpful to further understand the spatial distribution of various parameters involved in the corrosion process.

A feature analysis was performed to quantitatively compare the results between the present simulation images and experimentally corroded images. This type of comparison is similar to image processing techniques [21] for comparing two images. The experimental data (2-D corroded images) available for model validation were obtained from white-light interferometer microscopy at the Center for Materials Diagnostics at the University of Dayton Research Institute. Both histogram and wavelet feature analyses were carried out on simulated corrosion pit damage images and with the experimental data to validate the three-dimensional corrosion pit initiation and growth simulation model. The histogram features that we extracted from the corroded images are statistically based, for which the histogram of the image is considered to be the probability distribution of the pixel values. These features provide us the characteristic information of the pixel value distribution for the corrosion damage process. In addition to the histogram features (mean, standard deviation, skew, energy, and entropy), wavelet features are also extracted through a discrete wavelet transform applied on the simulated images. The singular value decomposition (SVD) features of the wavelet coefficient matrix A are extracted and used for comparison between experimental data and simulations.

To validate our model quantitatively, we simulated corrosion corresponding to the 2-D experimental data obtained by the Center for Material Diagnostics. Of the various features considered, we found that energy and entropy showed significance with various parameters in the corrosion damage process. Features were compared at several layers through the depth of the metal to check the consistency of corrosion growth intensity. The results of the features (energy vs entropy) comparison at the topmost layer for the simulated image at 100 cycles is shown in Fig. 4. It can be seen from Fig. 4 that the entropy and energy features are in good comparison with the experimental data (specimen TS 16). Similar results are obtained for other layers through the material thickness. It was observed that the scatter in the experimental data is very large. This is likely due to various parameters affecting the corrosion damage process and not knowing all the values of parameters in experiments.

In Fig. 5, the SVDs are compared at different layers for selected experimental data (specimen LS 08) with the simulated data from the model. It can be seen from Fig. 5 that the SVDs compare well to the experimental data for most of the layers throughout the metal. Also, the values of SVD decrease as the metal layers increase. Similarly, results of the entropy feature between the simulation and experiment are shown in Fig. 6. It can be seen from Fig. 6 that a good comparison between the simulation and experimental data is again found. Also, the entropy values decrease with increasing layers through the thickness of the metal. This observation is reasonable, because the

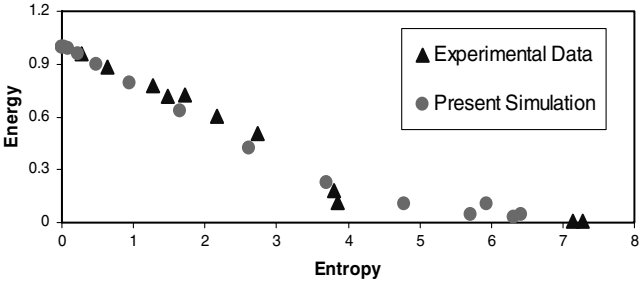


**Fig. 4 Comparison of extracted features between experimental data and the present simulation.**

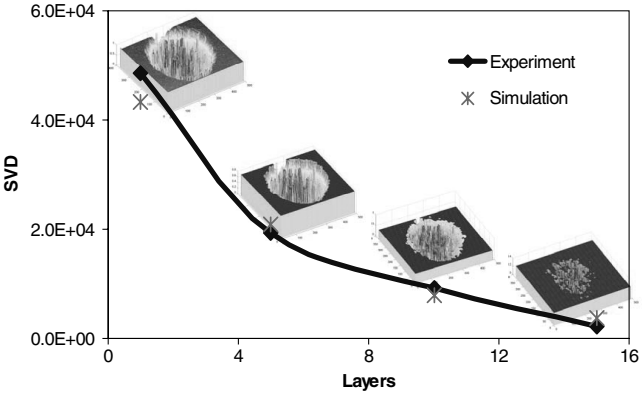


**Fig. 5 Comparison of extracted feature SVD from simulation with experimental data.**

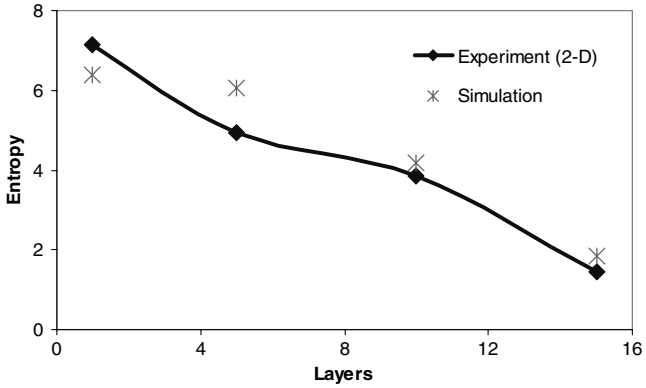


**Fig. 6 Comparison of extracted feature entropy from simulation with experimental data.**

randomness in corrosion is less in lower layers when compared with the top layer of the metal. Overall, the simulation results presented in Figs. 4–6 validate the corrosion damage process, giving the right trends from the simulation. More results of validation and effects of various electrochemical parameters and their sensitivity for 2-D corrosion initiation and growth can be found in Pidaparti et al. [22].

## Conclusions

A three-dimensional corrosion initiation and growth model for aircraft aluminum materials is developed. The model takes into account the electrochemical parameters and specific rules governing the corrosion mechanisms. The simulation program is implemented in a cellular automata framework and JAVA environment for ease of portability and usability. The corrosion initiation and growth patterns obtained from simulations are compared quantitatively with the experimental data, with reasonable agreement. However, many parameters affect the corrosion damage process, and more work is needed to validate computational models by conducting additional experiments. Currently, work is in progress to seek a more fundamental understanding of the macro- and microlevel corrosion growth and to model this based on local rules that can provide valuable information and tools for designing corrosion-resistant materials for a variety of applications.

## Acknowledgments

The authors thank the National Science foundation for funding this research through grants CMS-0516665 and DMR-0505039. The authors thank Chris Kacmar of the Center for Materials Diagnostics at the University of Dayton Research Institute for the experimental data used in the paper.

## References

[1] Wallace, W., and Hoeppner, D. W., "AGARD Corrosion Handbook," Vol. 1, AGARD, Rept. AG-278, July 1985.

[2] Strehblow, H. H., "Mechanisms of Pitting Corrosion," *Corrosion Mechanisms in Theory and Practice*, Marcel Dekker, New York, 1995, pp. 201–238.

[3] Marcus, P., and Oudar, J., (eds.), *Corrosion Mechanisms in Theory and Practice*, Marcel Dekker, New York, 1995.

[4] Wei, R. P., Liao, C. M., and Gao, M., "A Transmission Electron Microscopy Study of 7075-T6 and 2024-T3 Aluminum Alloys," *Metallurgical and Materials Transactions A: Physical Metallurgy and Materials Science*, Vol. 29, No. 4, 1998, pp. 1153–1160.

[5] Pao, P. S., Feng, C. R. J., and Gill, S. J., "Corrosion-Fatigue Crack Initiation in 7000-Series Al Alloys," *The Second Joint NASA/FAA/DoD Conference on Aging Aircraft*, No. 2, NASA Langley Research Center, Hampton, VA, 1999, pp. 831–840.

[6] Hoeppner, D. W., "Model for Prediction of Fatigue Lives Based Upon a Pitting Corrosion Fatigue Process," *Fatigue Mechanisms*, STP-675, American Society for Testing and Materials (ASTM), Philadelphia, 1979, pp. 841–863.

[7] Aziz, P. M., and Godard, H. P., "Pitting Corrosion Characteristics of Aluminum," *Industrial and Engineering Chemistry*, Vol. 44, 1952, 1791–1796.

[8] Frantiziskonis, G. N., Simon, L. B., Woo, J., and Matikas, T. E., "Multiscale Characterization of Pitting Corrosion and Application to an Aluminum Alloy," *European Journal of Mechanics, A/Solids*, Vol. 19, No. 2, 2000, pp. 309–317.

[9] Simon, L. B., Khobaib, M., Matikas, T. E., Jeffcoate, C. S., and Donley, M. S., "Influence of Pitting Corrosion on Structural Integrity of Aluminium Alloys," *Nondestructive Evaluation of Aging Materials and Composites 3*, Vol. 3585, SPIE—The International Society for Optical Engineering, Bellingham, WA, 1999, pp. 40–47.

[10] Macdonald, D. D., and Engelhardt, G., "Deterministic Prediction of Localized Corrosion Damage—A Reflective Review of Critical Issues," *The Journal of Corrosion Science and Engineering* [CD-ROM], Vol. 6, Inst. of Science and Technology, Univ. of Manchester, Manchester, England, U.K., 2003, Paper C065.

[11] Turnbull, A., "Review of Modeling Pit Propagation Kinetics," *British Corrosion Journal*, Vol. 28, No. 1, 1993, pp. 297–308.

[12] Wei, R. P., and Harlow, D. G., "A Mechanistically Based Probability Approach for Predicting Corrosion and Corrosion Fatigue Life," *Durability and Structural Integrity of Airframes*, edited by A. F. Blom, Engineering Materials Advisory Services, Warley, West Midlands, England, U.K., Vol. 1, pp. 347–366, June 1993.

[13] Harlow, D. G., and Wei, R. P., "A Probability Model for the Growth of Corrosion Pits in Aluminum Alloys Induced by Constituent Particles," *Engineering Fracture Mechanics*, Vol. 59, No. 3, 1998, pp. 305–325.

[14] Burstein, G. T., Liu, C., Souto, R. M., and Vines, S. P., "Origins of Pitting Corrosion," *Corrosion Engineering, Science and Technology*, Vol. 39, No. 1, 2004, pp. 25–31.

[15] Pidaparti, R. M., Palakal, M. J., and Fong, L., "A Cellular Automation Approach to Model Aircraft Corrosion Pit Damage Growth," *AIAA Journal*, Vol. 42, No. 12, 2004, pp. 2562–2569.

[16] Farmer, J. C., Bedrossian, P. J., and Mccright, R. D., "Modeling of Corrosion of High-Level Waste Containers CAM-CRM Interface," Univ. of California, Berkeley, Lawrence Livermore National Lab., Rept. UCRL-ID-129120, Berkeley, CA, 1998.

[17] Szklarska-Smialowska, Z., *Pitting Corrosion of Metals*, National Association of Corrosion Engineers, Houston, TX, 1986.

[18] Chopard, B., and Droz, M., *Cellular Automata Modeling of Physical Systems*, Cambridge Univ. Press, Cambridge, England, U.K., 1998.

[19] Wolfram, S., *Theory and Application of Cellular Automata*, World Scientific, Singapore, 1986.

[20] Wolfram, S., *Cellular Automata and Complexity*, Addison Wesley, Reading MA, 1994.

[21] Umbaugh, S., *A Practical Approach Using CVIP Tools*, Prentice–Hall, Upper Saddle River, NJ, 1998.

[22] Pidaparti, R. M., Puri, A., Palakal, M. J., and Kashyap, A., "Two-Dimensional Corrosion Pit Initiation and Growth Simulation Model," *Computers, Materials & Continua*, Vol. 2, No. 1, 2005, pp. 65–76.

R. Kapania
*Associate Editor*